Article

Structural Variation in Polyoxomolybdate Hybrid Crystals Comprising Ionic-Liquid Surfactants

Takeru Ito [1],*, Keisuke Mikurube [1], Kimiko Hasegawa [2], Takashi Matsumoto [2], Kurato Kosaka [1], Haruo Naruke [3] and Shinichi Koguchi [1]

[1] Department of Chemistry, School of Science, Tokai University, 4-1-1 Kitakaname, Hiratsuka 259-1292, Japan; E-Mails: k_m0423_tokai@yahoo.co.jp (K.M.); sttok413@gmail.com (K.K.); koguchi@tokai-u.jp (S.K.)

[2] X-ray Research Laboratory, Rigaku Corporation, 3-9-12 Matsubara-cho, Akishima 196-8666, Japan; E-Mails: kimiko@rigaku.co.jp (K.H.); t-matumo@rigaku.co.jp (T.M.)

[3] Chemical Resources Laboratory, Tokyo Institute of Technology, 4259-R1-23, Nagatsuta, Midori-ku, Yokohama 226-8503, Japan; E-Mail: hnaruke@gmail.com

* Author to whom correspondence should be addressed; E-Mail: takeito@keyaki.cc.u-tokai.ac.jp; Tel.: +81-463-58-1211 (ext. 3737); Fax: +81-463-50-2094.

Abstract: Polyoxomolybdate inorganic-organic hybrid crystals were synthesized with 1-decyl-3-methylimidazolium and 1-dodecyl-3-methylimidazolium as ionic-liquid surfactants. Both hybrid crystals possessed alternate stacking of surfactant layers and octamolybdate (Mo_8) monolayers, while the molecular structures of Mo_8 were different depending on the surfactants and solvents employed for crystallization. Each Mo_8 anion was connected by two sodium cations to form infinite one-dimensional chain. The surfactant chains in these crystals were arranged in a complicatedly bent manner, which will be induced by the weak C–H$\cdots$O hydrogen bonds between the Mo_8 anions and ionic-liquid surfactants.

Keywords: inorganic-organic; layered crystal; polyoxometalate; ionic-liquid; surfactant

1. Introduction

Ionic-liquids enable to construct hybrid materials with functions such as catalytic or conductive properties owing to their specific characteristics [1–4]. Inorganic-organic hybrid compounds using

ionic-liquid surfactants will exhibit higher structural variation than purely inorganic compounds and higher stability than purely organic compounds. In such ionic-liquid hybrids, the structures and arrangements of molecular components should be precisely controlled for the emergence of characteristic functions as realized in functional hybrid molecular conductors [5,6].

Polyoxometalate anions having physicochemical functions such as redox, catalytic or conductive properties [7–12] have been successfully organized by structure-directing surfactants to construct inorganic-organic hybrids [13–20] and layered crystals [21–30]. These polyoxometalate-surfactant hybrids allow flexible selection of the ionic components including ionic liquid [31–36], which leads to precise engineering of the structure and function.

We report here structural variation of polyoxomolybdate hybrid crystals synthesized by using long-tailed ionic-liquid surfactants. 1-decyl-3-methylimidazolium ($[(C_{10}H_{21})C_3H_3N_2(CH_3)]^+$, C_{10}im) and 1-dodecyl-3-methylimidazolium ($[(C_{12}H_{25})C_3H_3N_2(CH_3)]^+$, C_{12}im) were employed as cationic surfactants. Both crystals comprised octamolybdate ($Mo_8O_{26}^{4-}$, Mo_8) anion and sodium cation (C_{10}im-Na-Mo_8 and C_{12}im-Na-Mo_8). The weak interactions between poloxomolybdates and surfactants are considered to affect the formation of complicated packing structures.

2. Results and Discussion

2.1. Crystal Structure of C_{10}im-Na-Mo_8

C_{10}im-Na-Mo_8 was obtained from as-prepared hybrid composed of C_{10}im and polyoxomolybdate, which contained β-type octamolybdate (β-Mo_8) as in the case that C_{12}im was utilized [29]. C_{10}im-Na-Mo_8 crystals suitable for X-ray crystallography were obtained by employing 1-butanol (1-BuOH) as crystallization solvent.

The single crystal X-ray structure analysis combined with the elemental analysis revealed the formula of C_{10}im-Na-Mo_8 to be $[(C_{10}H_{21})C_3H_3N_2(CH_3)]_2Na_2[β-Mo_8O_{26}]$ 4[1-BuOH] (Table 1). Figure 1 shows the crystal structure of C_{10}im-Na-Mo_8. The crystal packing consisted of alternating β-Mo_8 inorganic layers and C_{10}im organic layers with periodicity of 19.6 Å (Figure 1b).

Two C_{10}im cations (1+ charge) and two Na^+ were associated with one β-Mo_8 anion (4− charge) due to the charge compensation. The inorganic layers were composed of infinite chains of β-Mo_8 connected by Na^+ along *b* axis (Figure 1c) as observed in β-Mo_8 crystals hybridized with hexadecylpyridinium ($[C_5H_5N(C_{16}H_{33})]^+$, C_{16}py) [27,28]. The space between the β-Mo_8-Na^+ chains were filled by imidazole rings of C_{10}im, which were located in the vicinity of Na^+ cations. The imidazole rings of C_{10}im had no π–π stacking interaction. C_{10}im-Na-Mo_8 contained two linker Na^+ per one β-Mo_8, while C_{16}py-Mo_8 had one linker Na^+ per one β-Mo_8. This difference may be due to the difference in the surfactant type (imidazolium or pyridinium). All 1-BuOH molecules of crystallization were bonded to Na^+ cations, and the 1-BuOH molecules were neutral as judged from the charge balance between the cations (two C_{10}im and two Na^+) and anion (one β-Mo_8).

Table 1. Crystallographic data.

Compound	$C_{10}im$-Na-Mo$_8$	$C_{12}im$-Na-Mo$_8$
Chemical formula	$C_{44}H_{55}N_4Na_2Mo_8O_{30}$	$C_{44}H_{94}N_4Na_2Mo_8O_{30}$
Formula weight	1933.43	1972.73
Crystal system	monoclinic	triclinic
Space group	$P2_1/n$ (No. 14)	$P\bar{1}$ (No. 2)
a (Å)	20.089 (4)	9.5496 (6)
b (Å)	8.8791 (18)	11.3505 (8)
c (Å)	39.931 (9)	16.8466 (12)
α (°)	–	102.283 (8)
β (°)	100.301 (3)	90.927 (7)
γ (°)	–	104.802 (8)
V (Å^3)	7008 (3)	1720.2 (3)
Z	4	1
ρ_{calcd} (g cm^{-3})	1.832	1.904
T (K)	93	93
μ (Mo Kα) (mm^{-1})	1.472	1.500
No. of reflections measured	70784	21352
No. of independent reflections	15939	7869
R_{int}	0.0874	0.0536
No. of parameters	730	381
R_1 ($I > 2\sigma(I)$)	0.0933	0.0494
wR_2 (all data)	0.2612	0.1276

The organic layers were constructed from decyl groups of $C_{10}im$ cations and butyl groups of 1-BuOH molecules to form bilayer-like structure (Figure 1b). However, these decyl and butyl chains were not interdigitated. Each $C_{10}im$ cation had two *gauche* C–C bonds in the decyl chain [C7–C8 and C11–C12; C21–C22 and C25–C26 (C26–C27B)], while the other C–C bonds had *anti* conformation (Figure 1a). The $C_{10}im$ cations had complicatedly bent conformation in their chain structure. The presence of more than two *gauche* C–C bonds per one alkyl chain was rarely observed for polyoxometalate-surfactant hybrid crystals [21–30]. The C–C bonds in the butyl groups had *anti* conformation.

The bent $C_{10}im$ cations had several weak C–H···O hydrogen bonds [37] (Figure 2). The hydrogen bonds were formed mainly at the interface between the β-Mo$_8$ and $C_{10}im$ layers. In addition, some C–H···O bonds were present in the vicinity of the *gauche* C–C bonds. The C···O distance was in the range of 3.11–3.78 Å (mean value: 3.40 Å). The *gauche* C–C bonds near the end of decyl chain [C11–C12 and C25–C26 (C26–C27B)] had weak C···C interactions between other decyl and butyl chains.

2.2. Crystal Structure of $C_{12}im$-Na-Mo$_8$

$C_{12}im$-Na-Mo$_8$ was obtained from as-prepared hybrid of $C_{12}im$-Mo$_8$ containing β-Mo$_8$ [29]. Suitable crystals of $C_{12}im$-Na-Mo$_8$ were obtained from ethanol solution under the presence of Na$^+$ or Li$^+$, while $C_{12}im$-β-Mo$_8$ without Na$^+$ was crystallized from acetonitrile [29].

Figure 1. Crystal structure of C_{10}im-Na-Mo$_8$. H atoms are omitted for clarity. (**a**) Asymmetric unit drawn by displacement ellipsoids at the 30% probability level. Minor parts of the disordered C atoms are indicated in transparent color; (**b**) Packing diagram along *b* axis (Mo$_8$ in polyhedral representations); (**c**) Molecular arrangements in the inorganic layers. The decyl and butyl groups are omitted for clarity.
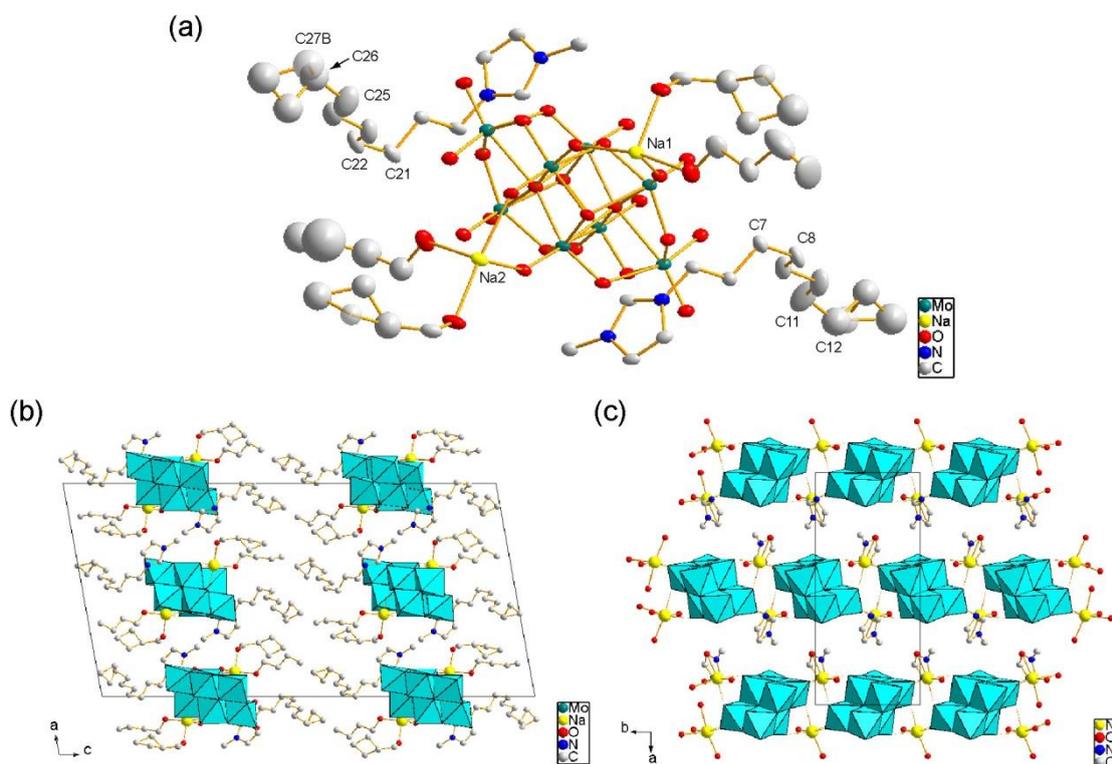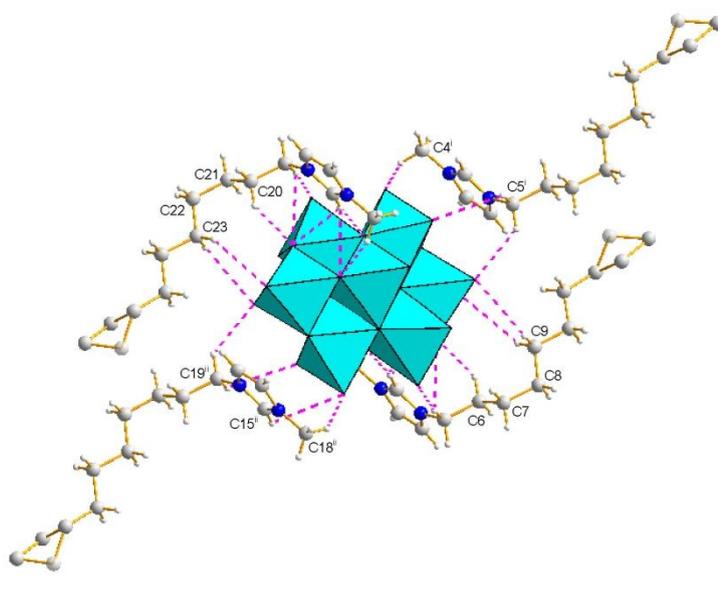

Figure 2. C–H$\cdots$O hydrogen bonds in C_{10}im-Na-Mo$_8$ (pink dotted line). Selected hydrogen bonds between Mo$_8$ moiety and C_{10}im are represented [symmetry code: (i) *x*, −1 + *y*, *z*; (ii) *x*, 1 + *y*, *z*]. Na$^+$ and 1-BuOH are omitted for clarity. Minor parts of the disordered C atoms are indicated in transparent color.

The formula of $C_{12}im$-Na-Mo_8 was revealed to be $[(C_{12}H_{25})C_3H_3N_2(CH_3)]_2Na_2[\gamma\text{-}Mo_8O_{24}(OC_2H_5)_4]$ $2C_2H_5OH$ (Table 1). The anion was γ-type Mo_8 coordinated by four ethoxo ligands (Figure 3a) [38–41]. The dissolved β-Mo_8 from as-prepared $C_{12}im$-Mo_8 reacted with ethanol to isomerize into ethoxo-grafted γ-Mo_8 anions, which reprecipitated as $C_{12}im$-γ-Mo_8 crystals. The crystal structure of $C_{12}im$-Na-Mo_8 was composed of alternating Mo_8 inorganic layers and $C_{12}im$ organic layers with periodicity of 16.4 Å (Figure 3b).

Figure 3. Crystal structure of $C_{12}im$-Na-Mo_8. H atoms are omitted for clarity. (**a**) Asymmetric unit together with atoms generated by the symmetry operation to complete Mo_8 anion [symmetry code: (i) $-x$, $-y$, $-z$]; Displacement ellipsoids are drawn at the 50% probability level; (**b**) Packing diagram along *b* axis (Mo_8 in polyhedral representations); (**c**) Molecular arrangements in the inorganic layers. The dodecyl and ethyl groups are omitted for clarity.
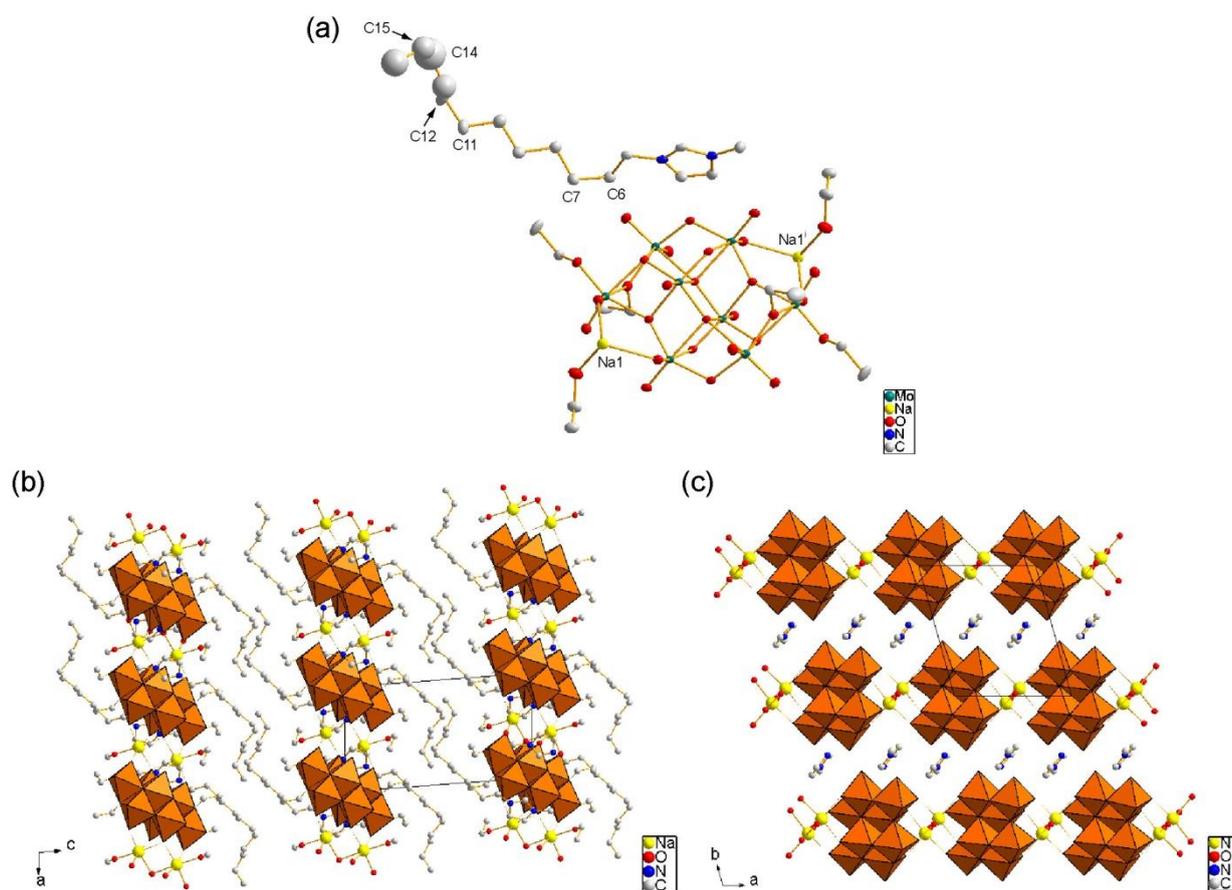

Two $C_{12}im$ cations (1+ charge) and two Na^+ were associated with one γ-Mo_8 anion (4− charge). The inorganic layers were composed of infinite chains of γ-Mo_8 connected by two linker Na^+ cations along *a* axis (Figure 3c), being similar to $C_{10}im$-Na-Mo_8. The space between the γ-Mo_8-Na^+ chains are filled by imidazole rings of $C_{12}im$, which are located in the vicinity of Na^+ cations. The imidazole rings of $C_{12}im$ were parallel, but no π–π stacking interaction was observed. One neutral EtOH molecule of crystallization was bonded to each Na^+ cation.

The organic layers were composed of dodecyl groups of $C_{12}im$ cations (Figure 3b). The dodecyl chains were bent without interdigitation, being different from other polyoxometalate-surfactant hybrid

crystals comprising interdigitated straight surfactant chains. Each C_{12}im cation had three *gauche* C–C bonds (C6–C7, C11–C12, and C14–C15), resulting in the bent chain conformation of C_{12}im as in the case of C_{10}im-Na-Mo_8.

The complicatedly bent C_{12}im cations had several weak C–H⋯O hydrogen bonds [37] with γ-Mo_8 anions (Figure 4). The hydrogen bonds were formed mainly at the interface between the γ-Mo_8 and C_{12}im layers, and some C–H⋯O bonds were present in the vicinity of *gauche* C–C bonds. The C⋯O distance was in the range of 2.96–3.70 Å (mean value: 3.32 Å). The *gauche* C–C bonds (C14–C15) near the end of dodecyl chain had weak C⋯C interactions between other dodecyl chains and ethyl groups. In addition, there were weak interactions between γ-Mo_8 and ethoxo groups of γ-Mo_8 (intramolecular C–H⋯O hydrogen bonds) and between γ-Mo_8 and ethanol connected to Na^+ (intremolecular C–H⋯O hydrogen bonds).

Figure 4. C–H⋯O hydrogen bonds in C_{12}im-Na-Mo_8 (pink dotted line). Selected hydrogen bonds between Mo_8 moiety and C_{12}im are represented [symmetry code: (ii) *x*, −1 + *y*, *z*]. Na^+, ethyl groups, and EtOH are omitted for clarity.
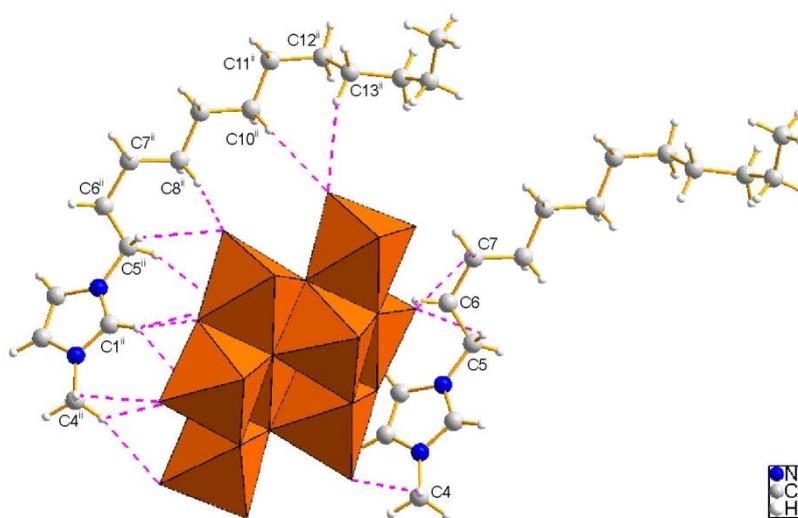
3. Experimental Section

3.1. Syntheses and Methods

All chemical reagents except for imidazolium surfactants were obtained from commercial sources (Wako, Osaka, Japan). As-prepared C_{10}im-Mo_8 was precipitated by adding ethanol solution of C_{10}im·Br (0.2 M, 10 mL) [42] to Na_2MoO_4·$2H_2O$ aqueous solution (0.5 M, 10 mL), which was adjusted to pH 3.8 with 6 M HCl. Colorless needle crystals of C_{10}im-Na-Mo_8 were obtained from 1-BuOH/acetonitrile (13 mL/2 mL) solution of the as-prepared C_{10}im-Mo_8 hybrid (0.10 g) and NaCl (0.02 g) kept at 303–308 K (yield: 21% based on Mo). Some 1-BuOH molecules of crystallization seem to be exchanged with acetonitrile. Anal.: Calculated for $C_{44}H_{90}N_6Na_2Mo_8O_{29}$: C: 26.68%, H: 4.58%, N: 4.24%. Found: C: 27.08%, H: 4.08%, N: 4.34%. Melting point: 463 K. Infrared (KBr disk): 1165 (w), 937 (s), 914 (s), 901 (m), 839 (m), 707 (s), 669 (m), 619 (w), 577 (w), 555 (w), 525 (w), 480 (w), 453 (w), 413 (m) cm^{-1}.

As-prepared $C_{12}im$-Mo_8 hybrid, a starting precipitate for $C_{12}im$-Na-Mo_8 crystals, was obtained according to the literature [29]. Colorless plate crystals of $C_{12}im$-Na-Mo_8 were crystallized from ethanol (15 mL) solution of the as-prepared $C_{12}im$-Mo_8 hybrid (0.05 g) containing $NaNO_3$ or $LiNO_3$ (0.02–0.03 g) (yield: 15% based on Mo). Some ethoxo ligands of $C_{12}im$-Na-Mo_8 were probably exchanged for hydroxo ligands by the reaction with water in the air, which seems to cause the isomerization of γ-Mo_8 to β-Mo_8. Anal.: Calculated for $C_{32}H_{66}N_4Na_2Mo_8O_{28}$: C: 21.73%, H: 3.76%, N: 3.17%. Found: C: 21.27%, H: 3.32%, N: 3.06%. Melting point: 509 K. Infrared (KBr disk): 1167 (w), 1120 (w), 1054 (w), 937 (s), 914 (s), 900 (m), 841 (m), 710 (s), 669 (w), 659 (w), 620 (w), 554 (w), 534 (w), 522 (w), 499 (w), 474 (m), 437 (w), 425 (m), 413 (w), 405 (w) cm^{-1}.

3.2. X-Ray Crystallography

Single crystal X-ray diffraction measurements were performed on a Rigaku Saturn724 diffractometer with multi-layer mirror monochromated Mo-Kα radiation (λ = 0.71075 Å) (Rigaku, Tokyo, Japan). Diffraction data were collected and processed with CrystalClear [43]. The structure was solved by direct methods [44] for $C_{10}im$-Na-Mo_8 and by heavy-atom Patterson methods for $C_{12}im$-Na-Mo_8 [45]. The refinement procedure was performed by the full-matrix least-squares using SHELXL97 [46]. All calculations were performed using the CrystalStructure [47] software package. Most non-hydrogen atoms were refined anisotropically, while the rest were refined isotropically. The hydrogen atoms on C atoms were refined using the riding model. $C_{10}im$-Na-Mo_8 crystals were very fine needles, and the weak reflection intensities may result in relatively high R_1 and wR_2 values. In the refinement of $C_{10}im$-Na-Mo_8 structure, the hydrogen atoms relevant to the disordered C atoms and on O atoms of 1-BuOH were not included. In the refinement of $C_{12}im$-Na-Mo_8 structure, a hydrogen atom attached to the O atom of ethanol was found in the difference Fourier synthesis and their positional and isotropic displacement parameters were refined. Further details of the crystal structure investigation may be obtained free of charge from the Cambridge Crystallographic Data Centre, 12 Union Road, Cambridge CB2 1EZ, UK; Fax: (+44)-1223-336-033; or E-Mail: deposit@ccdc.cam.ac.uk (CCDC 980232 and 980233).

4. Conclusions

The hybrid crystals composed of polyoxomolybdate and imidazolium ionic-liquid surfactants, $[(C_{10}H_{21})C_3H_3N_2(CH_3)]_2Na_2[β\text{-}Mo_8O_{26}]$ 4[1-BuOH] ($C_{10}im$-Na-Mo_8) and $[(C_{12}H_{25})C_3H_3N_2(CH_3)]_2Na_2$ $[γ\text{-}Mo_8O_{24}(OC_2H_5)_4]$ $2C_2H_5OH$ ($C_{12}im$-Na-Mo_8), were synthesized. Both hybrid crystals contained octamolybdate (Mo_8) anions associated with Na^+ to form one-dimensional Mo_8-Na^+ chain, although the molecular structures of Mo_8 were different (β-Mo_8 for $C_{10}im$-Na-Mo_8 and ehoxo-modified γ-Mo_8 for $C_{12}im$-Na-Mo_8). The crystal structures comprised alternate stacking of Mo_8 monolayers and surfactant layers. Both crystals contained complicatedly bent conformation in the surfactant chain, which is considered to be derived from the weak C–H···O hydrogen bonds. These ionic-liquid hybrid crystals are expected to exhibit specific catalytic property such as esterification, oxidation, or phase transfer catalysis, and to exhibit Na^+-ion conductivity.

Acknowledgments

Conflicts of Interest

The authors declare no conflict of interest.

References

1. Welton, T. Room-temperature ionic liquids. Solvents for synthesis and catalysis. *Chem. Rev.* **1999**, *99*, 2071–2083.
2. Wasserscheid, P.; Keim, W. Ionic liquids-new "solutions" for transition metal catalysis. *Angew. Chem. Int. Ed.* **2000**, *39*, 3772–3789.
3. Haumann, M.; Riisager, A. Hydroformylation in room temperature ionic liquids (RTILs): Catalyst and process developments. *Chem. Rev.* **2008**, *108*, 1474–1497.
4. Honma, I.; Yamada, M. Bio-inspired membranes for advanced polymer electrolyte fuel cells. Anhydrous proton-conducting membrane via molecular self-assembly. *Bull. Chem. Soc. Jpn.* **2007**, *80*, 2110–2123.
5. Coronado, E.; Gómez-García, C.J. Polyoxometalate-based molecular materials. *Chem. Rev.* **1998**, *98*, 273–296.
6. Coronado, E.; Giménez-Saiz, C.; Gómez-García, C.J. Recent advances in polyoxometalate-containing molecular conductors. *Coord. Chem. Rev.* **2005**, *249*, 1776–1796.
7. Pope, M.T. *Heteropoly and Isopoly Oxometalates*; Springer: Berlin, Germany, 1983.
8. Hill, C.L. Introduction: Polyoxometalates multicomponent molecular vehicles to probe fundamental issues and practical problems. *Chem. Rev.* **1998**, *98*, 1–2.
9. Long, D.-L.; Burkholder, E.; Cronin, L. Polyoxometalate clusters, nanostructures and materials: From self assembly to designer materials and devices. *Chem. Soc. Rev.* **2007**, *36*, 105–121.
10. Proust, A.; Matt, B.; Villanneau, R.; Guillemot, G.; Gouzerh, P.; Izzet, G. Functionalization and post-functionalization: A step towards polyoxometalate-based materials. *Chem. Soc. Rev.* **2012**, *41*, 7605–7622.
11. Okuhara, T.; Mizuno, N.; Misono, M. Catalytic chemistry of heteropoly compounds. *Adv. Catal.* **1996**, *41*, 113–252.
12. Sadakane, M.; Steckhan, E. Electrochemical properties of polyoxometalates as electrocatalysts. *Chem. Rev.* **1998**, *98*, 219–237.
13. Song, Y.-F.; Long, D.-L.; Ritchie, C.; Cronin, L. Nanoscale polyoxometalate-based inorganic/organic hybrids. *Chem. Rec.* **2011**, *11*, 158–171.
14. Qi, W.; Wu, L. Polyoxometalate/polymer hybrid materials: Fabrication and properties. *Polym. Int.* **2009**, *58*, 1217–1225.

15. Clemente-León, M.; Coronado, E.; Soriano-Portillo, A.; Mingotaud, C.; Dominguez-Vera, J.M. Langmuir–Blodgett films based on inorganic molecular complexes with magnetic or optical properties. *Adv. Colloid Interface Sci.* **2005**, *116*, 193–203.

16. Stein, A.; Fendorf, M.; Jarvie, T.P.; Mueller, K.T.; Benesi, A.J.; Mallouk, T.E. Salt-gel synthesis of porous transition-metal oxides. *Chem. Mater.* **1995**, *7*, 304–313.

17. Janauer, G.G.; Dobley, A.; Guo, J.; Zavalij, P.; Whittingham, M.S. Novel tungsten, molybdenum, and vanadium oxides containing surfactant ions. *Chem. Mater.* **1996**, *8*, 2096–2101.

18. Taguchi, A.; Abe, T.; Iwamoto, M. Non-silica-based mesostructured materials: Hexagonally mesostructured array of surfactant micelles and 11-tungstophosphoric heteropoly anions. *Adv. Mater.* **1998**, *10*, 667–669.

19. Landsmann, S.; Lizandara-Pueyo, C.; Polarz, S. A new class of surfactants with multinuclear, inorganic head groups. *J. Am. Chem. Soc.* **2010**, *132*, 5315–5321.

20. Zhang, G.; Ke, H.; He, T.; Xiao, D.; Chen, Z.; Yang, W.; Yao, J. Synthesis and characterization of new layered polyoxometallates-1,10-decanediamine intercalative nanocomposites. *J. Mater. Res.* **2004**, *19*, 496–500.

21. Janauer, G.G.; Dobley, A.D.; Zavalij, P.Y.; Whittingham, M.S. Evidence for decavanadate clusters in the lamellar surfactant ion phase. *Chem. Mater.* **1997**, *9*, 647–649.

22. Spahr, M.E.; Nesper, R. Anhydrous octamolybdate with trimethyl hexadecyl ammonium cations. *Z. Anorg. Allg. Chem.* **2001**, *627*, 2133–2138.

23. Nyman, M.; Ingersoll, D.; Singh, S.; Bonhomme, F.; Alam, T.M.; Brinker, C.J.; Rodriguez, M.A. Comparative study of inorganic cluster-surfactant arrays. *Chem. Mater.* **2005**, *17*, 2885–2895.

24. Nyman, M.; Rodriguez, M.A.; Anderson, T.M.; Ingersoll, D. Two structures toward understanding evolution from surfactant-polyoxometalate lamellae to surfactant-encapsulated polyoxometalates. *Cryst. Growth Des.* **2009**, *9*, 3590–3597.

25. Yin, P.; Wu, P.; Xiao, Z.; Li, D.; Bitterlich, E.; Zhang, J.; Cheng, P.; Vezenov, D.V.; Liu, T.; Wei, Y. A double-tailed fluorescent surfactant with a hexavanadate cluster as the head group. *Angew. Chem. Int. Ed.* **2011**, *50*, 2521–2525.

26. Ito, T.; Sawada, K.; Yamase, T. Crystal structure of bis(dimethyldioctadecylammonium) hexamolybdate: A molecular model of Langmuir-Blodgett films. *Chem. Lett.* **2003**, *32*, 938–939.

27. Ito, T.; Mikurube, K.; Abe, Y.; Koroki, T.; Saito, M.; Iijima, J.; Naruke, H.; Ozeki, T. Hybrid inorganic-organic crystals composed of octamolybdate isomers and pyridinium surfactant. *Chem. Lett.* **2010**, *39*, 1323–1325.

28. Ito, T.; Mikurube, K.; Hasegawa, K.; Kurasawa, M.; Naruke, H.; Ozeki, T. Polyoxomolybdate-surfactant hybrid layered crystal with unusually long periodicity. *Chem. Lett.* **2011**, *40*, 626–628.

29. Ito, T.; Ide, R.; Kosaka, K.; Hasegawa, S.; Mikurube, K.; Taira, M.; Naruke, H.; Koguchi, S. Polyoxomolybdate-surfactant layered crystals derived from long-tailed alkylamine and ionic-liquid. *Chem. Lett.* **2013**, *42*, 1400–1402.

30. Ito, T. Polyoxometalate-surfactant hybrids as building strategy for two-dimensional molecular arrays. *Polyoxometalate Chem.* **2012**, *1*, 6–14.

31. Bourlinos, A.B.; Raman, K.; Herrera, R.; Zhang, Q.; Archer, L.A.; Giannelis, E.P. A liquid derivative of 12-tungstophosphoric acid with unusually high conductivity. *J. Am. Chem. Soc.* **2004**, *126*, 15358–15359.

32. Leng, Y.; Wang, J.; Zhu, D.; Ren, X.; Ge, H.; Shen, L. Heteropolyanion-based ionic liquids: Reaction-induced self-separation catalysts for esterification. *Angew. Chem. Int. Ed.* **2009**, *48*, 168–171.

33. Rafiee, E.; Evani, S. Polyoxometalate-based acid salts with tunable separation properties as recyclable Brönsted acid catalysts for the synthesis of β-keto enol ethers. *Catal. Commun.* **2012**, *25*, 64–68.

34. Chen, X.; Souvanhthong, B.; Wang, H.; Zheng, H.; Wang, X.; Huo, M. Polyoxometalate-based ionic liquid as thermoregulated and environmentally friendly catalyst for starch oxidation. *Appl. Catal. B* **2013**, *138–139*, 161–166.

35. Jiang, Y.; Liu, S.; Li, S.; Miao, J.; Zhang, J.; Wu, L. Anisotropic ionic liquids built from nonmesogenic cation surfactants and Keggin-type polyoxoanions. *Chem. Commun.* **2011**, *47*, 10287–10289.

36. Rickert, P.G.; Antonio, M.R.; Firestone, M.A.; Kubatko, K.-A.; Szreder, T.; Wishart, J.F.; Dietz, M.L. Tetraalkylphosphonium polyoxometalate ionic liquids: Novel, organic-inorganic hybrid materials. *J. Phys. Chem. B* **2007**, *111*, 4685–4692.

37. Desiraju, G.R.; Steiner, T. *The Weak Hydrogen Bond in Structural Chemistry and Biology*; Oxford University Press: New York, NY, USA, 1999; pp. 12–16.

38. McCarron, E.M., III; Harlow, R.L. Synthesis and structure of $Na_4[Mo_8O_{24}(OCH_3)_4]$ 8MeOH: A novel isopolymolybdate that decomposes with the loss of formaldehyde. *J. Am. Chem. Soc.* **1983**, *105*, 6179–6181.

39. Niven, M.L.; Cruywagen, J.J.; Heyns, J.B.B. The first observation of γ-type octamolybdates: Synthesis, crystal and molecular structure of $[Me_3N(CH_2)_6NMe_3]_2[Mo_8O_{26}]$ $2H_2O$. *J. Chem. Soc. Dalton Trans.* **1991**, *20*, 2007–2011.

40. Inoue, M.; Yamase, T. Synthesis and crystal structures of γ-type octamolybdates coordinated by chiral lysines. *Bull. Chem. Soc. Jpn.* **1995**, *68*, 3055–3063.

41. Khan, M.I.; Zubieta, J. Oxovanadium and oxomolybdenum clusters and solids incorporating oxygen-donor ligands. *Prog. Inorg. Chem.* **1995**, *43*, 1–149.

42. Aupoix, A.; Pégot, B.; Vo-Thanh, G. Synthesis of imidazolium and pyridinium-based ionic liquids and application of 1-alkyl-3-methylimidazolium salts as pre-catalysts for the benzoin condensation using solvent-free and microwave activation. *Tetrahedron* **2010**, *66*, 1352–1356.

43. *CrystalClear*; Rigaku Corporation: Tokyo, Japan, 1999.

44. Altomare, A.; Cascarano, G.; Giacovazzo, C.; Guagliardi, A.; Burla, M.; Polidori, G.; Camalli, M. *SIR*92—A program for automatic solution of crystal structures by direct methods. *J. Appl. Cryst.* **1994**, *27*, 435–436.

45. Beurskens, P.T.; Admiraal, G.; Beurskens, G.; Bosman, W.P.; Garcia-Granda, S.; Gould, R.O.; Smits, J.M.M.; Smykalla, C. *The DIRDIF Program System*; University of Nijmegen: Nijmegen, The Netherlands, 1992.

46. Sheldrick, G.M. A short history of SHELX. *Acta Cryst. Sect. A* **2007**, *64*, 112–122.
47. *Crystal Structure 4.0*; Rigaku Corporation: Tokyo, Japan, 2010.